FINITE ELEMENT ANALYSIS OF COMPATIBILITY METRICS IN FRONTAL COLLISIONS

Pradeep Mohan
FHWA/NHTSA National Crash Analysis Center,
The George Washington University,
David L. Smith
National Highway Traffic Safety Administration (NHTSA)
United States of America
Paper Number 07-0188

ABSTRACT

Several numeric measures have been proposed to assess crash compatibility between two vehicles. The measures under investigation in this study are the Average Height of Force 400 (AHOF400) and the Crush-Work Stiffness 400 (Kw400), both measured in 35 mph full-frontal rigid load cell barrier tests. AHOF400 is a measure of the vertical centroid of forces exerted on the barrier surface for the first 400 mm of crush. Kw400 is a measure of the work required to crush 400 mm of a vehicle's front end.

Several studies in the past have concluded that there are large inherent errors in the AHOF measure. One of the main factors influencing the error in this measure is the size of the load cell on the barrier face. In this study, different barrier concepts are examined which can reduce or eliminate the dependency of AHOF400 on load cell size. A finite element analysis was used as a basis to recommend a barrier design that can accurately measure AHOF400. In addition, the influence of impact speed and vehicle mass on AHOF400 and Kw400 are discussed.

Due to the errors associated with the height of force measurement, the relationship between occupant injury measures and height of force matching in the light vehicle crash data is not well understood. The barrier proposed in this study, which eliminates the error in the AHOF400 measure, will enable us to better understand the effects of height of force matching in the vehicle fleet.

INTRODUCTION

In recent years, the trend of growing sales of sport utility vehicles (SUVs) and pick-up trucks, generally referred to as Light Trucks and Vans (LTVs), has led to renewed public attention on the crash compatibility issue. This issue has been discussed by several researchers [1-5]. It has been generally agreed that the crash incompatibility between vehicles be attributed to three vehicle factors: (1) mass incompatibility (2) stiffness incompatibility and (3) geometry incompatibility.

Mass has a strong influence on the level of compatibility of two vehicles involved in a collision. Due to the fact that the change in momentum of each body involved in a collision is equal, the lighter body experiences a higher change in velocity during the collision [6]. However, in this study, mass was treated as a condition of the crash and not as a design variable.

Stiffness compatibility is a complex issue. Several studies have tried to establish a relationship between mass and stiffness [7-9]. These studies have shown a weak correlation between mass and stiffness, thus indicating that mass and stiffness are independent vehicle characteristics. Achieving stiffness compatibility is a challenging goal, given the possible goal conflict between self and partner protection, especially for the heavier vehicles.

Front-end geometry influences the potential for structural interaction in a car-to-car collision. Improving the geometric compatibility is the most feasible first step to improve vehicle crash compatibility. Vehicle geometry can be varied, within limits, independent of vehicle mass [6].

This study provides an engineering analysis for quantifying stiffness and geometry metrics to assess vehicle compatibility in frontal crashes.

COMPATIBILITY METRICS

Worldwide research is ongoing to quantify a vehicle's structure through a dynamic performance test and associated metrics to balance the aggressivity/vulnerability across the vehicle fleet [10]. The metrics under consideration in this study are the Crush-Work Stiffness 400 (Kw400) and Average Height of Force 400 (AHOF400), both measured in 35 mph full-frontal rigid load cell barrier tests.

Stiffness Metric

The stiffness metric referred to as Crush-Work Stiffness (Kw400) is derived from equating ideal spring energy to the work of crushing the vehicle front end [9]. Kw400 is the symbol for a metric that comes from the integral of the area under the force-displacement curve evaluated between 25 to 400 mm of front-end crush as illustrated in the first equation below.

$$\int_{25}^{400} F dx = \frac{1}{2} Kw400[(400)^2 - (25)^2]$$

$$F(400-25) = \frac{1}{2} Kw400[(400)^2 - (25)^2]$$

$$Kw400 = \frac{2F}{425}$$

Here, F is the average of the total force exerted on the rigid barrier wall between 25 and 400 mm of vehicle crush. Thus, Kw400 is directly proportional to amount of energy it takes to crush the vehicle front end. A low Kw400 is a soft vehicle, and high Kw400 is a stiff vehicle.

The first 25 mm of crush is ignored intentionally in the Kw400 calculation. This is due to several factors such as soft materials in the initial crush, the noise and the cross-talk in the measured data and the distortions caused by the band-pass filter that is traditionally used in processing crash test data. Therefore the calculations are not begun until the vehicle crush reaches 25 mm. The maximum crush is limited to 400 mm to isolate the high inertial forces on the load cell wall due to engine contact.

Force was obtained from the load cell array placed on the rigid wall for research purposes during the US New Car Assessment Program (USNCAP) tests. Displacement was obtained from double integrating the acceleration measured from the accelerometers placed at the front seat cross-members. Both force and acceleration were sampled at 10 KHz. But, once force is cross-plotted vs. displacement, the F-d curve is no longer at a fixed step size as displacement is a non-linear function of time. The force-displacement data were re-sampled with a fixed step size in displacement before computing average force F to avoid errors in the Kw400 measure.

To illustrate the Kw400 calculation, consider two NCAP tests as shown in figure 1. Test 5303 is the NCAP test of an SUV and test 5326 is the NCAP test of a compact car. The force-displacement curves for the two tests are shown in Figure 1. Kw400 calculated for these two vehicles using the above method is shown in Figure 2.

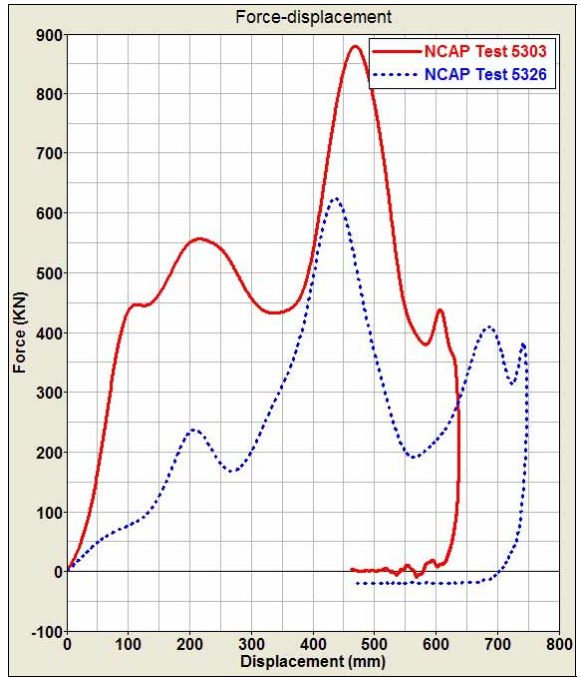

Figure 1. Force-displacement curves for an SUV and a compact car.

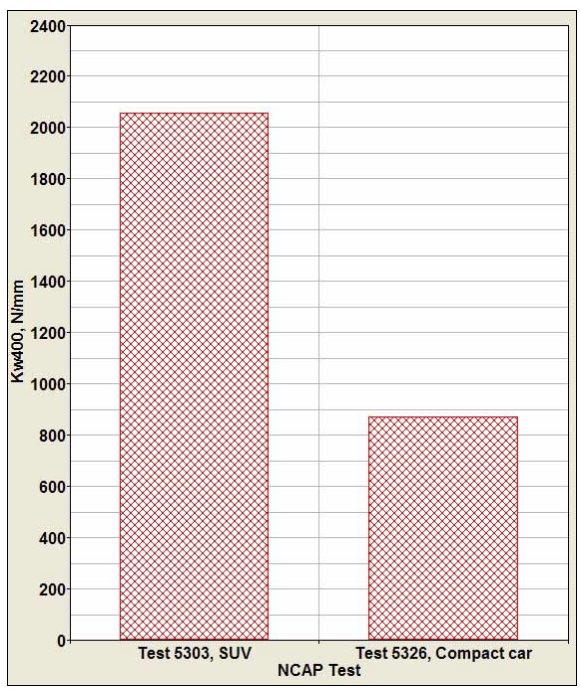

Figure 2. Kw400 for an SUV and a compact car.

Geometry Metric

The geometry metric referred to as the AHOF400 is derived from the height at which the vehicle imparts force to the rigid wall. When a vehicle hits the load cell barrier in a full frontal impact, the individual forces measured on the array of load cells are used to calculate the Height of Force (HOF). Each of the load cell forces, F, from the load cell wall at a given time are multiplied by their respective height from the ground, summed, and then divided by the sum of all the forces as illustrated in Figure 3. In the HOF equation, "n" represents the number of load cells and "d" represents the vehicle crush. The AHOF400 is the weighted average of the HOF values during the first 25 to 400 mm of vehicle crush as illustrated in the below equation. The first 25 mm of crush is ignored intentionally in the AHOF400 calculation for the same reasons explained earlier.

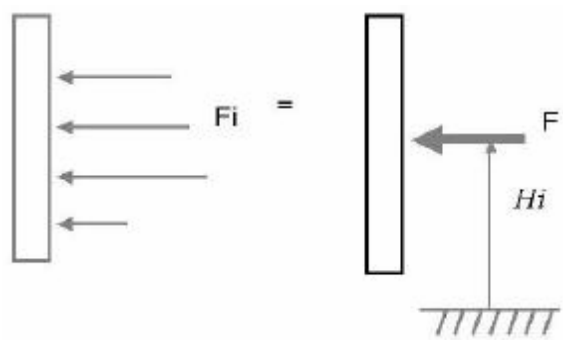

$$HOF(d) = \frac{\sum_{i=1}^{n} F_i(d) H_i(d)}{\sum_{i=1}^{n} F_i(d)}$$

$$AHOF_{crush} = \frac{\sum_{d=25mm}^{400mm} HOF(d) F(d)}{\sum_{d=25mm}^{400mm} F(d)}$$

Figure 3. Height of force calculation.

Several studies in the past have concluded that there are large inherent errors in the AHOF measure [11-14]. In the current frontal USNCAP testing, the full-width rigid barrier is instrumented with single-axis load cells. The HOF measured in these tests has a large source of error.

For example, consider a force, F_X, applied at the lower most point on the surface of the single-axis load cell of size d as shown in Figure 4. As illustrated in the Figure, the force measured by the single-axis load cell is assumed to be at its center irrespective of the actual position of the applied force. Thus, using single-axis load cells, the error in height of force measurement could be as high as ½ the load cell size. One of the main factors influencing the error in height of force measurement using single-axis load cells is the size of the load cell on the barrier face [15].

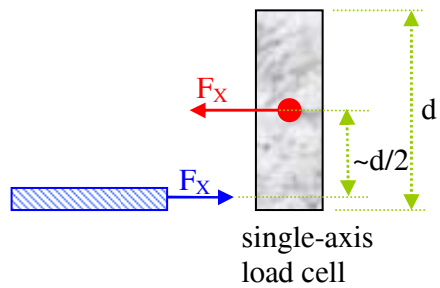

Figure 4. Measurement error in single-axis load cells.

RESULTS AND DISCUSSION

Finite element simulations using LS-DYNA were conducted to evaluate the error content in the AHOF400 computed from rigid wall data and also robustness of the AHOF400 and Kw400 metrics. Three different vehicle Finite Element (FE) models (1996 Dodge Neon, 2003 Ford Explorer and 1999 Dodge Caravan) shown in Figure 5 were used in this study. These vehicle models were chosen so as to represent different class of vehicles in the current US vehicle fleet. These models have been previously validated to a full frontal USNCAP test and the validation reports are available for download from the NCAC website.

http://www.ncac.gwu.edu/vml/models.html

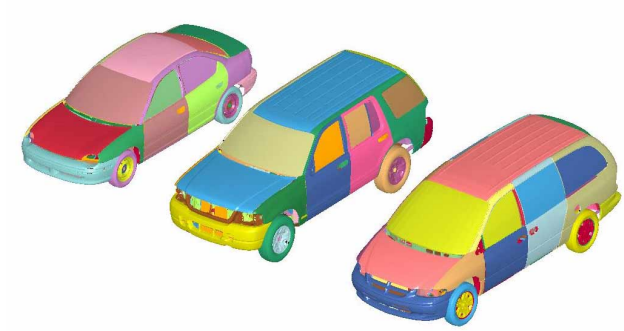

Figure 5. Vehicle FE models (Neon, Explorer and Caravan).

As discussed above, the accuracy of the AHOF400 is dependent on the size of the axial load cells used to measure the HOF. In order to avoid this problem in simulation studies, the true AHOF400 was computed for the three vehicle models using a single load cell on the rigid wall as illustrated in Figure 6. The load cell used here measured force in the impact direction and also the moment about the y-axis as a function of the applied force. By using this load cell it was possible to locate the exact location of force on the vertical axis, thus leading to a precise estimate of the AHOF400.

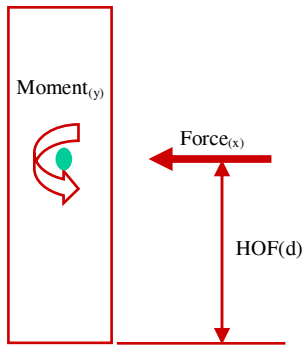

$$\mathbf{HOF\ (d)} = \frac{\mathbf{Moment_{(y)}\ (d)}}{\mathbf{Force_{(x)}\ (d)}}$$

Figure 6. True/Actual AHOF400 calculation.

True AHOF400 computed for the three vehicle models is shown in Figure 7. A current industry proposal for a voluntary matching zone for geometrically compatible vehicles is the Part 581 low speed bumper zone that spans from 16 inches (406.4 mm) to 20 inches (508 mm) above the ground [16]. This zone could provide for common interaction of vehicles and needs special attention for the collection of height data and the matching of height metrics like AHOF400.

Figure 7. True/Actual AHOF400 comparison.

METRICS ROBUSTNESS STUDY

Real world crashes occur at a wide range of impact speeds, vehicle masses and depend on several other variables. No two real world crashes are identical. A metric chosen to define a compatible vehicle should not heavily depend on these variables under nominal conditions. Several simulation studies were conducted to evaluate the influence of impact speed and vehicle mass on AHOF400 and Kw400.

Influence of Impact Speed on AHOF400

In addition to the USNCAP simulation, two additional finite element simulations were conducted for the three vehicle types at 30 and 40 mph. The vehicle components, predominantly steel structures, exhibit strain rate effects. This means, the stress at which yield occurs is dependent on the rate of deformation. These rate effects have been included in the vehicle models to ensure accurate prediction of the crash response at different impact speeds [17, 18]. True AHOF400 was computed for each of these simulations using the method explained earlier. The variation in AHOF400 for the three vehicles at three different speeds is shown in Figure 8. The minimum and maximum AHOF400 was 442 mm and 453 mm respectively for the Dodge Neon. Minute variations in AHOF400 were observed for the other vehicle types as well at the different impact speeds. Based on the simulation results, it was concluded that impact speed has negligible effect on this measure.

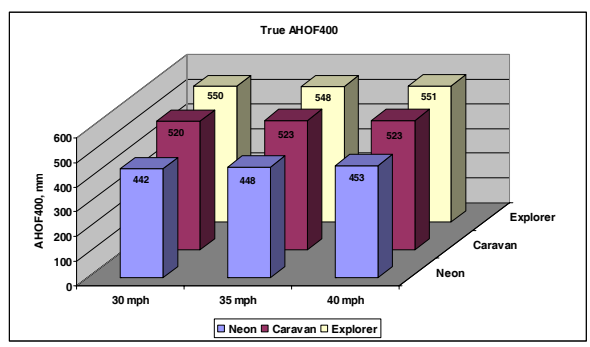

Figure 8. Influence of impact velocity on AHOF400.

Influence of Vehicle Mass on AHOF400

The next step in this study was to understand the influence of vehicle mass on AHOF400. The three vehicle models were massed incrementally to different level of occupancy starting from the unloaded vehicle weight. These masses were rigidly attached to the vehicle at the designated seating positions. Table 1 shows the mass increments

considered for the Dodge Neon, which were incremented above the unloaded design weight (UDW). Similar mass increments were considered for the Ford Explorer and Dodge Caravan. With each mass increment there will be minor change in ride heights of the vehicle. The ride height difference was not considered in this study as there was no accurate way of determining the effect of mass on ride height of these vehicles, especially using crash based finite element vehicle models. Simulations were conducted for these five mass increments using USNCAP test conditions. The simulation results showed that mass has negligible influence on AHOF400. The force-deflection curves were identical for the first 400 mm of crush in each of these simulations. Based on this study, it was concluded that AHOF400 is a function of the vehicle design. Assuming the change in ride height is negligible, added vehicle mass and speed have negligible effect on this metric.

Table 1.
Mass increments for Dodge Neon

	UDW (kg)	Number of occupants	Total Mass (kg)
Dodge Neon	1155	1	1231
		2	1307
		3	1383
		4	1459
		5	1535

Influence of Impact Speed on Kw400

The Kw400 for the three vehicle models was calculated using the method explained earlier and is shown in Figure 9, note that these results are for the 35 mph impact speed.

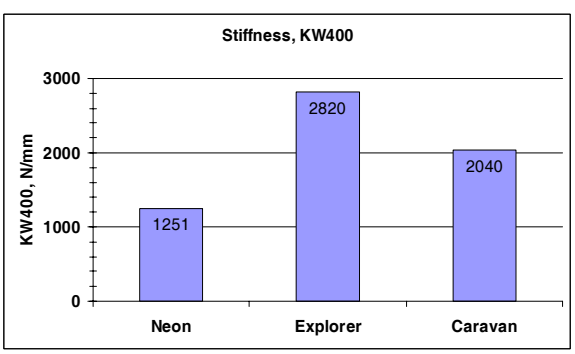

Figure 9. Kw400 comparison.

Finite Element simulations were conducted at 30, 35 and 40 mph to determine the influence of impact speed on Kw400 metric. The variation of Kw400 for the three vehicle models at different impact speeds is shown in Figure 10. The maximum variation of Kw400 with impact speed was 22% for the Dodge Neon, 32.5% for the Dodge Caravan and 13.5% for the Ford Explorer.

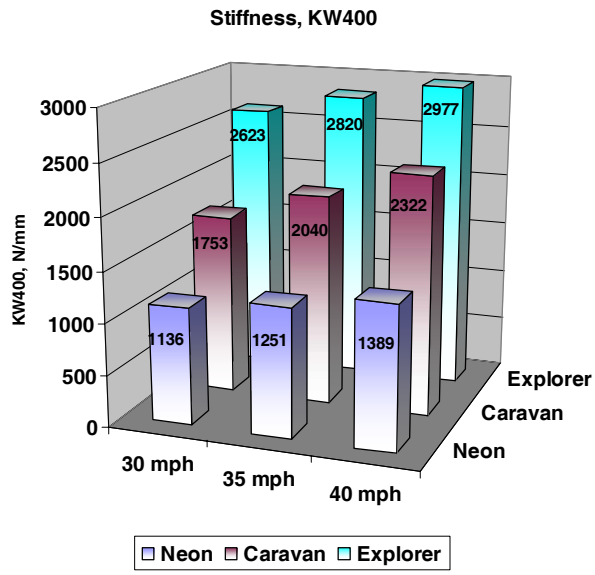

Figure 10. Influence of impact velocity on Kw400.

To further examine this variation, consider the force-displacement curves for the Ford Explorer and Dodge Caravan shown in Figures 11 and 12. The F-d curves for the Ford Explorer showed similar response until the vehicle experienced about 350 mm of crush at the three impact speeds. The overall vehicle crush reached only 400 mm at 30 mph impact speed. At 35 mph impact, the kinetic energy increased to 1.36 times to that of the 30 mph impact. At 40 mph the increase in kinetic energy was 1.77 times. To satisfy the principle of conservation of energy, the vehicle had to absorb more energy at 35 and 40 mph respectively. This is accomplished by reaching higher crush levels, thus increasing the energy absorbed by the vehicle at higher speeds. An interesting thing to note in these Figures is that the F-d curves for the Dodge Caravan start deviating earlier, at about 150 mm of crush, when compared to the Ford Explorer. The overall crush in the Dodge Caravan reached 535 mm at 30 mph. Due to higher kinetic energy at 35 and 40 mph the Dodge Caravan reached crush levels of 630 mm and 730 mm, respectively. The Dodge Caravan is a unibody construction and has multiple load paths which highly influence the force-displacement characteristics at different impact speeds. The Ford Explorer, on the other hand, is body-on-frame type construction. Since the frame rails form the primary load path in this type of construction, the F-d curves showed little variation up to 350 mm of crush. Based on the above observations, it was concluded that the

vehicle design and impact speed has a strong influence on Kw400.

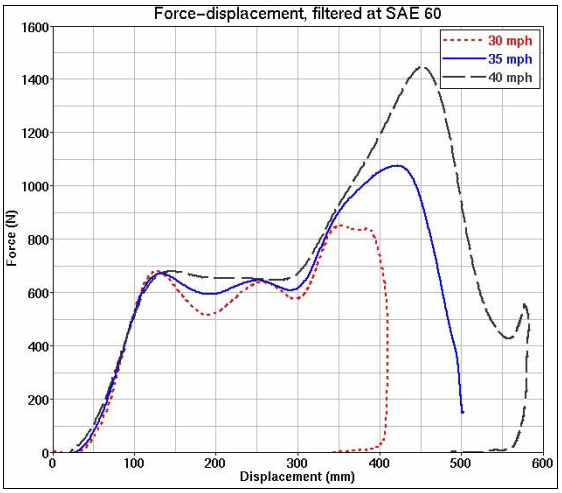

Figure 11. FE force-displacement curves for Ford Explorer at three different impact velocities.

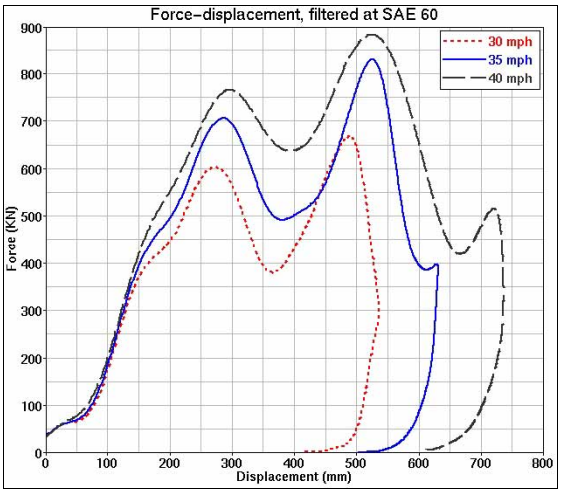

Figure 12. FE force-displacement curves for Dodge Caravan at three different impact velocities.

At higher closing speeds, the Kw400 for each of the vehicle models increased. This shows that the work done to reach the 400 mm crush level increased as the impact speed increased. In a two-vehicle crash, the relative size of the metrics is critical. Thus, the ratio of the stiffness metrics should remain constant as the crash speed is varied in order for this metric to be useful. Under this consideration, the Explorer/Neon stiffness ratio is seen to be 2.31, 2.25, and 2.14 as the test speed is varied from 30 to 40 mph. Similarly, the Caravan/Neon stiffness ratio is seen to be 1.54, 1.63, and 1.67 as the speed is increased. These ratios show good consistency across the range of energy conditions studied and thus indicate good usefulness.

Influence of Vehicle Mass on Kw400

In order to determine the influence of vehicle mass on Kw400, the vehicle models were massed incrementally to different levels of occupancy starting from the unloaded vehicle weight. Again, these masses were added to the vehicle so as to represent the occupied seating position. Table 2 summarizes the mass increments considered for the Dodge Neon.

Table 2.
Kw400 for Dodge Neon at Different Mass Increments

	UDW (kg)	Number of occupants	Total Mass (kg)	Kw400 (N/mm)
Dodge Neon	1155	1	1231	1261.2
		2	1307	1260.1
		3	1383	1249.2
		4	1459	1247.9
		5	1535	1250.9

The total mass rose from 1231 Kg with one occupant to 1535 Kg with five, a 25% increase. The force-displacement curves for these simulations are shown in Figure 13. The change in kinetic energy with different mass increments showed no noticeable difference in the force-displacement curves in the Kw400 evaluation region of 400 mm vehicle crush. Overall vehicle crush slightly increased with increased kinetic energy. For each of these cases the value of Kw400 was computed according to the method described earlier. The lowest value computed was 1247.9 N/mm and the highest was 1261.2. The maximum variation was about 1%.

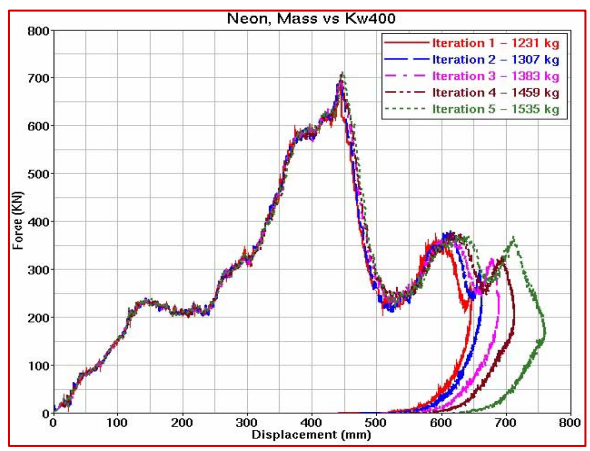

Figure 13. FE force-displacement curves for Dodge Neon at different mass increments.

A similar study of added mass was conducted for the Ford Explorer. Table 3 summarizes the mass increments considered. The mass increase was about 15%, the total mass increased from 2116 Kg with one occupant to 2420 Kg with five. The maximum variation in the Kw400 measure was about 1%. This is a negligible variation in computed values.

Table 3.
Kw400 for Ford Explorer at Different Mass Increments

	UDW (kg)	Number of occupants	Total Mass (kg)	Kw400 (N/mm)
Ford Explorer	2040	1	2116	2828.2
		2	2192	2827.8
		3	2268	2820.7
		4	2344	2812.9
		5	2420	2800.1

From this study, the simulation results suggested that Kw400 is predominantly a function of vehicle design. Added vehicle mass under nominal conditions was shown to have no influence on this metric. Kw400 does show some dependence on impact speed, but this effect seems to be similar for all vehicles so stiffness ratios remain fairly constant. This needs to be further investigated.

BARRIER DESIGN

The next step in this study was to determine a rigid barrier design that provides the data required to accurately compute the height of force and stiffness data needed. Full width rigid load cell barrier concepts were proposed based on a load cell resolution study [15]. Since the part 581 zone spans about 100 mm vertically, it was critical to locate the exact HOF for fleet matching as proposed by the Alliance voluntary agreement. [16]. For an assumed 10% error allowance, only $\pm$ 10 mm error would be allowed for this zone. However, the load cell resolution study showed that the error in AHOF400 measurement was greater than 10mm unless 62.5 mm single-axis square load cells were used to instrument the barrier. Further, this did not eliminate the error altogether. Earlier in the paper (figure 6) the need for an added moment channel (My) to accurately measure HOF was discussed. To this end, 4 barrier concepts and variants of those with multi-axis load cells are considered for the cost analysis. The following criteria were considered in proposing these concepts:

- Barrier length and width to fit all previous frontal NCAP vehicles
- Possibility of calculating International Research Harmonization Activity (IHRA) recommended compatibility metrics [19]
- Ability to accurately compute AHOF400 and analyze forces distribution in the Part 581 zone.

The Concept 1 barrier was instrumented with five rows and nine columns of 250x250 mm load cells (Fx and My) and is shown in Figure 14. A ground clearance of 80 mm was chosen for the barrier such that the Part 581 zone lies in the center of the 2nd row of load cells. This barrier is similar to the barrier used in conjunction with USNCAP except that multi-axis load cells are used instead of single-axis load cells. An additional row and column have been added to accommodate the larger SUVs and pickups anticipated in future USNCAP tests.

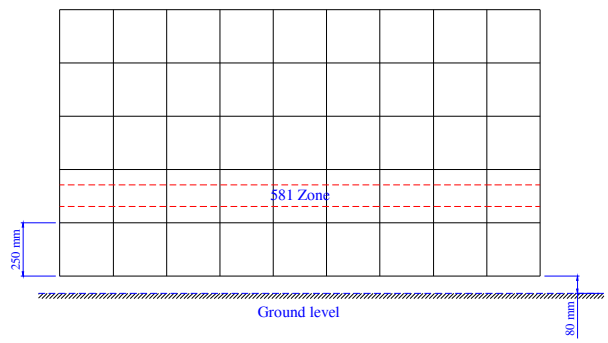

Figure 14. Barrier concept 1.

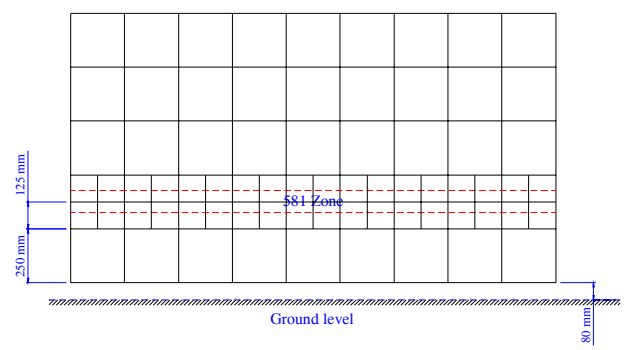

Figure 15. Barrier concept 2.

The Concept 2 barrier was instrumented with 250x250 mm load cells (Fx and My) throughout except for the 2nd & 3rd rows. This area is defined as the "Common Interaction Zone" among European researchers. The 2nd and 3rd rows are instrumented with 125 mm load cells (Fx only), which are placed with respect to the Part 581 zone according to the positions for the IHRA barrier and would allow limited comparison of data internationally in this region. This concept is shown in Figure 15. Concept

2a is similar to concept 2. The only difference is that, multi-axis load cells are used to instrument the rigid barrier in the common interaction zone instead of single-axis load cells.

The Concept 3 barrier is similar to Concept 2 barrier. It is instrumented with 250x250 mm load cells (Fx and My) throughout except for the 2nd & 3rd row. The 2nd and 3rd rows are instrumented with 100 mm load cells (Fx only) to give clear coverage to the Part 581 zone. The ground clearance had to be adjusted to 56.4 mm such that the 3rd row of load cells overlaps the Part 581 zone. This concept is shown in Figure 16. Concept 3a is similar to concept 3. The only difference is that, multi-axis load cells are used through out to instrument the rigid barrier instead of single-axis load cells.

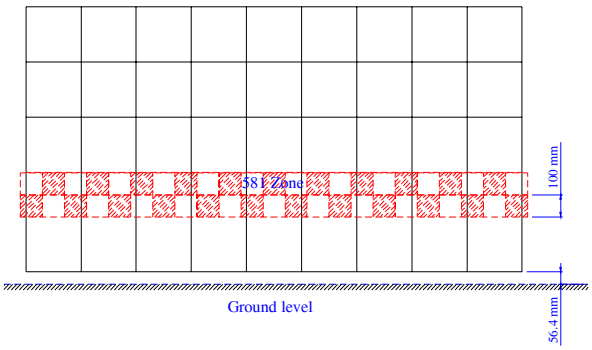

Figure 16. Barrier concept 3.

The Concept 4 barrier is instrumented with 125x125 mm load cells (Fx only) throughout and is shown in Figure 17. The load cells in this concept are the same size as those used by IHRA and other international bodies, though the load cells in those barriers are covered with 2 layers of deformable honeycomb. This configuration would allow the best possible sharing of data between NHTSA and the international test and evaluation community. Concept 4a is similar to concept 4. The only difference is that, multi-axis load cells (Fx and My) are used to instrument the rigid barrier instead of single-axis load cells.

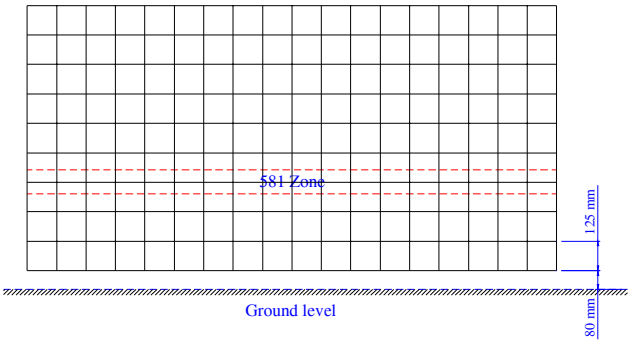

Figure 17. Barrier concept 4.

Barrier Selection Criteria

Several variants of these proposed concept barriers with single-axis and multi-axis load cells were considered in the cost/benefit study. The barrier selection and recommendation was based on the following criteria:

- Accuracy in measuring AHOF400
- Possibility of measuring HNT/VNT (horizontal and vertical structural distributions) as proposed by IHRA [19]
- Initial cost of the barrier
- Cost of test data collection per test
- Cost of quality control per test

While a 9x18 load cell array measuring axial force only does not have the accuracy needed for AHOF400 metrics [15], it is nevertheless included in several cases for cost comparison purposes. Appendix A summarizes the cost/benefit study for different barrier concepts and its variants.

Budgetary quotes were obtained from 4 load cell manufacturers active in the crash testing field. The current cost of test data collection per channel is $23 and the cost of quality control per channel is $4. These costs are the same for all barriers, but the number of data channels makes a great difference to overall costs.

Concept barrier 1 is sufficient and necessary to accurately measure AHOF400. The initial cost to purchase this barrier is comparable to some of the other concepts. Further, the cost/test with this barrier concept is lower compared to other concepts because it has fewer data channels. However, this barrier was not recommended as it does not provide an opportunity to gather data required to compute IHRA recommended compatibility metrics.

Barrier concept 4a was recommended based on the findings of this study for two reasons. First, this barrier can accurately measure AHOF400 compared to the IHRA barrier, which could not. Second, if NHTSA decides to harmonize the compatibility tests with IHRA and international stakeholders, a deformable layer of honeycomb can be added to this barrier in order to measure the distribution type compatibility metrics defined by IHRA. The only shortcoming of this barrier is the added data channels required in each test. This adds the cost of test data collection and quality control to the cost of each test.

Further, these additional data channels add to the initial cost of the barrier, though the initial cost estimates varied widely from comparable to other designs to much more expensive. Subsequent conversations with load cell manufacturers have indicated that several testing facilities are interested in this barrier concept, some are purchasing and some are awaiting NHTSA's purchase decision.

CONCLUSIONS

AHOF400 and Kw400 were analyzed as metrics that could capture the key vehicle compatibility characteristics of height of force and energy absorption in the frontal compartment, respectively. AHOF400 ensures that the vehicle structures engage properly, reducing under ride and override. Kw400 ensures that the crash energy is properly shared between the impacting vehicles.

The dependence of AHOF400 and Kw400 metrics on impact speed and vehicle mass was investigated through computer simulations. Three different impact speeds (30, 35 and 40 mph) were considered. Five different mass increments were evaluated at the NCAP test condition. The results of these simulations showed that vehicle mass and impact speed under nominal conditions have no influence on AHOF400. Although vehicle mass showed no influence on Kw400, it did show some dependence on impact speed. Nevertheless, stiffness ratios show good constancy across a wide range of crash energy and should be investigated further.

Several finite element studies were performed to lay a basis for improved barrier design and a best concept to meet multiple criteria was selected. The load cells that are used to instrument the rigid barrier should measure a minimum of two channels (X-force and Y-moment as a function of the applied force) to accurately locate the height of force. The new barrier proposed in this study is expected to create better source data for accurate height of force estimates.

REFERENCES

[1] Gabler, H. C. and Hollowell, W. T., "NHTSA's Vehicle Aggressivity and Compatibility Research Program", Proceedings of the Sixteenth International Enhanced Safety of Vehicle Conference, Paper No. 98-S3-O-01, Windsor, Canada (1998)

[2] Gabler, H. C. and Hollowell W. T., "The Aggressivity of Light Trucks and Vans in Traffic Crashes", Society of Automotive Engineers Paper No. 980908, February 1998

[3] Summers, S., Hollowell, W.T., Prasad, A., "NHTSA's Research Program for Vehicle Compatibility", 18th International Conference on the Enhanced Safety of Vehicles, Paper 307, May 2003.

[4] Verma, M.K., Lavelle J., Lange R.C., "Perspectives on Vehicle Crash Compatibility and Relationship to Other Safety Criteria", 18th International Conference on the Enhanced Safety of Vehicles, Paper 412, May 2003.

[5] Reilly, P.O., "Status Report of IHRA Compatibility and Frontal Impact Working Group", 18th International Conference on the Enhanced Safety of Vehicles, Paper 402, May 2003.

[6] Thomas, G., Zobel, R., Schwarz, T., "Required Measures to Improve the Structural Interaction Potential of Passenger Cars", Society of Automotive Engineers, Paper No. 2005-01-1351, March 2005.

[7] Nusholtz, G., Rabbiolo, G., and Shi, Y., "Estimation of the Effects of Vehicle Size and Mass on Crash-Injury Outcome through Parameterized Probability Manifolds", Society of Automotive Engineers, Paper no 2003-01-0905, March 2003.

[8] Mizuno, K., Kajzer, J., "Compatibility Problems in Frontal, Side, Single Car Collisions and Car-to-Pedestrian Accident in Japan", Accident Analysis and Prevention, Pages 381-391, 1998.

[9] Nusholtz, G., et al "Vehicle Mass, Stiffness and their Relationship", Twentieth International Technical Conference on the Enhanced Safety of Vehicles, Paper No. 05-0413, 2005.

[10] Mizuno, K., Tateishi, K., Ezaka, Y., "Test Procedures to Evaluate Vehicle Compatibility", Seventeenth International Technical Conference on the Enhanced Safety of Vehicles, Paper No. 127, Amsterdam, 2001.

[11] Verma, M. K., Nagappala, R., et al "Significant Factors in Height of Force Measurements for Vehicle Collision Compatibility", Society of Automotive Engineers, Paper No. 2004-01-1165, March 2004.

[12] Jerinsky, M., Hollowell, T., "NHTSA's Review of Vehicle Compatibility Performance Metric Through Computer

Simulation", ASME International Mechanical Engineering Congress and Exposition, Paper Number IMECE2003-44045, Washington, D.C., 2003.

[13] Takizawa, S., Sugimoto, T., Suzuki, K., "A Study of Compatibility Test Procedure in Frontal Impact", 18th ESV, Paper Number 437, Nagoya, 2002.

[14] Jerinsky, M., Hollowell, T., "NHTSA's Review of High-Resolution Load Cell Wall's Role in Designing for Compatibility", 18th ESV, Paper Number 393, Nagoya, 2003.

[15] Mohan, P., Marzougui, D., Kan, C.D., "Modified Approach to Accurately Measure Height of Force (HOF)", Society of Automotive Engineers, Paper Number 2007-01-1182, April 2007.

[16] Barbat, S., "Status of Enhanced Front-to-Front Vehicle Compatibility Technical Working Group Research and Commitments", 19th ESV, Paper Number 05-0463, Washington D.C, 2005.

[17] Simunovic, S., Nukala, V., et al., "Modeling of Strain Rate Effects in Automotive Impact", Soceity of Automotive Engineers, Paper No. 2003-01-1383, March 2003.

[18] Xu, K., Wong, C., et al., "High Strain Rate Constitutive Model for High Strength Steels", Soceity of Automotive Engineers, Paper No. 2003-01-0260, March 2003.

[19] O'Reilly, P., "Status Report of IHRA Compatibility and Frontal Impact Working Group," 19th ESV, Paper Number 05-0365, Washington D.C, 2005.

APPENDIX A – LOAD CELL BARRIER COST/BENEFIT STUDY

	Crash wall description	Accuracy in measuring AHOF400	Ability to calculate HNT/VNT	Budgetary quotes from load cell manufacturer's				Cost of data collection per test	Number of channels for QC	Cost of QC/test
				1	2	3	4	$23/channel		$4/channel
Concept 1	250 mm LC (Fx & My)	Highly accurate	Not possible	$548K	$234K	$316K	$322K	$2,070	90	$360
Concept 2	250 mm LC (Fx & My), 125 mm LC (Fx)	Error due to single-axis LC in rows 2 and 3. This error could be as high as 1/2 the loadcell size (62.5 mm)	Can be computed based on IHRA's definition	$622K	$241K	$443K	$330K	$2,484	108	$432
Concept 2a	250 mm LC (Fx & My), 125 mm LC (Fx & My)	Highly accurate	Can be computed based on IHRA's definition	$664K	$324K	$458K	$347K	$3,312	144	$576
Concept 3	250 mm LC (Fx & My), 100 mm LC (Fx)	Error due to single-axis LC in rows 2 and 3. This error could be as high as 1/2 the loadcell size (50 mm)	Not possible	$628K	$256K	$472K	$356K	$2,714	118	$472
Concept 3a	250 mm LC (Fx & My), 100 mm LC (Fx & My)	Highly accurate	Not possible	$680K	$362K	$491K	$374K	$3,772	164	$656
Concept 4	125 mm LC (Fx)	Error due to single-axis LC. This error could be as high as 1/2 the loadcell size (62.5 mm)	Can be computed based on IHRA's definition	$286K	$243K	$863K	$310K	$3,726	162	$648
Concept 4a	125 mm LC (Fx & My)	Highly accurate	Can be computed based on IHRA's definition	$437K	$616K	$932K	$374K	$7,452	324	$1,296

VEHICLE-TO-VEHICLE FRONT-TO-SIDE CRASH ANALYSIS USING A CAE BASED METHODOLOGY

Saeed Barbat, Xiaowei Li and Priya Prasad
Passive Safety Research and Advanced Engineering
Ford Motor Company
United States
Paper Number 07-0347

ABSTRACT

Fundamental physics and numerous field studies have clearly shown a higher fatality risk for occupants in smaller and lighter vehicles when colliding with the heavier one, especially when the struck vehicle is a passenger car and the striking vehicle is an LTV or an SUV. The consensus is that the significant parameters influencing compatibility in front-to-side crashes are geometric interaction, vehicle stiffness, and vehicle mass. The effect of each individual design parameter, however, is not clearly understood.

A finite element (FE) model-based design of experiments (DOE) methodology focused on evaluating the effects of a few striking vehicle design variables on dummy responses of the struck vehicle in front-to-side impact was developed. This study utilized a deterministic approach including optimally spaced Latin hypercube sampling which allowed analytical prediction equations for dummy responses to be generated from twenty-one simulation runs. Selected response variables were the dummy injury measures Thoracic Trauma Index (TTI) and pelvis acceleration.

Several multi-dimensional response surfaces were constructed based on the simulation results and found to be well correlated (R^2= 0.83 and R^2=0.94 for TTI and pelvis acceleration, respectively). Results indicate that lower front-end structures in vehicle-to-vehicle front-to-side collisions have the greatest effect on reducing (struck vehicle driver) TTI than other design variables. This was found to contrast the pelvic acceleration results, which tended to increase with lower front structure height of the striking vehicle. The stiffness and mass showed moderate significance on the TTI with less mass effect than stiffness. The mass showed no significant effect on the pelvis acceleration.

1. INTRODUCTION

Vehicle compatibility has been investigated in many studies using different approaches such as real-world crash statistics, crash testing, and computer modeling. NHTSA used U.S. crash statistics from the Fatality Analysis Reporting System (FARS) to determine the number of fatalities in vehicle-to-vehicle collisions [1]. Field data analysis shows that side impact can be severe, harm producing crashes, even though they occur less frequently than frontal impacts [2]. Inherent design differences between utility vehicles and pickups, on one hand, and passenger cars, on the other, may lead to a higher fatality risk for occupants in passenger cars when colliding with the utility or pickups. This is commonly attributed to differences in geometry, relative masses, and relative stiffnesses between these two vehicle segments.

The Insurance Institute of Highway Safety (IIHS) reported a series of crash tests to assess the influence of mass, stiffness, and vehicle ride height on occupant responses, but the results were somewhat inconclusive [3]. Separating the effects of the compatibility factors via experimentation would not only be costly and time consuming, but also susceptible to systemic errors due to test-to-test variability. Because of the limitations of statistical approaches and physical crash testing, math models in combination with design of experiments (DOE) methods were deemed necessary.

Past studies of compatibility by the authors have addressed front-to-front compatibility. Barbat, *et al.* [4, 5] investigated factors influencing compatibility in frontal SUV/LTV-to-car crashes. Their study proposed a robust and repeatable vehicle-to-vehicle test procedure to assess vehicle compatibility and to extract individual effect of the compatibility factors on the injury outcome of occupants. Their results indicated that the geometric compatibility was the dominant factor influencing injury outcome in frontal vehicle-to-vehicle crashes.

Finite element (FE) simulations have been used to study many aspects of vehicle crashworthiness. Carefully designed experiments (partially factorial) can characterize responses over a selected design space using a reduced number of simulations (as compared to full-factorial study). In this study, the authors used a very similar approach to that reported

by Barbat et. al. [6], which reported on front-to-front compatibility. The application of this methodology was extended to investigate the effect of compatibility factors in front-to-side impact.

A FE model-based DOE methodology focused on evaluating the effects of a few design variables on dummy responses in front-to-side vehicle crash has been developed. The striking vehicle was selected to be an SUV while the struck vehicle was a mid size passenger car. The current study utilizes a deterministic approach that allowed analytical prediction equations for dummy responses to be generated. This study combined FE analysis, Latin Hyper Cube Sampling (LHS), and subset selection with sequential replacement to produce a powerful tool that may be used to investigate vehicle compatibility issues.

2. FINITE ELEMENT MODELING

Reliable finite element models of the vehicles are required to enable reasonable predictions of structural performance. In this study, a baseline front-to-side vehicle-to-vehicle FE model was constructed and correlated to a physical vehicle-to-vehicle front-to-side crash test. As in the physical test, the simulated passenger vehicle was stationary and the simulated SUV was given an initial velocity of 48kph (See Figure 1).

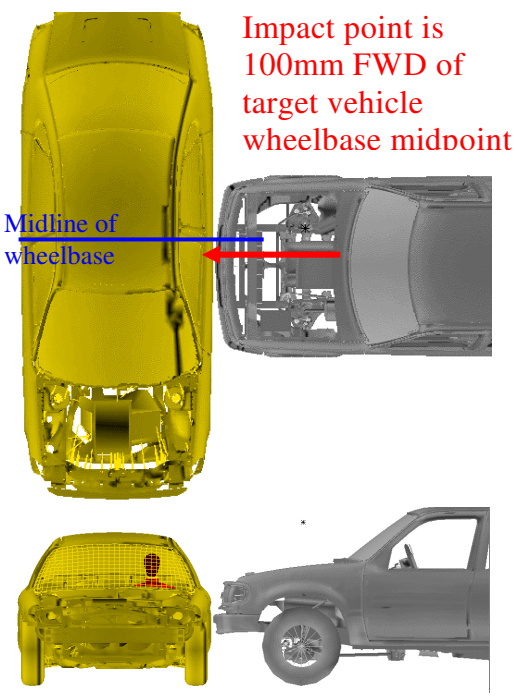

Figure 1. Impact configuration of an SUV-to-Car in front-to-side simulation.

Front-to-side SUV-to-passenger car simulations involve many complex and non-linear interactions. The nonlinear, explicit FE crash code, RADIOSS [7], was used for all of the simulations. The simulated structural deformation and side intrusion of the struck vehicle in a front-to-side SUV-to-passenger car impact were well correlated with test observations, as shown in Figures 2 and 3.

Figure 2. Validation of the deformation of struck vehicle in SUV-to-Car side impact.

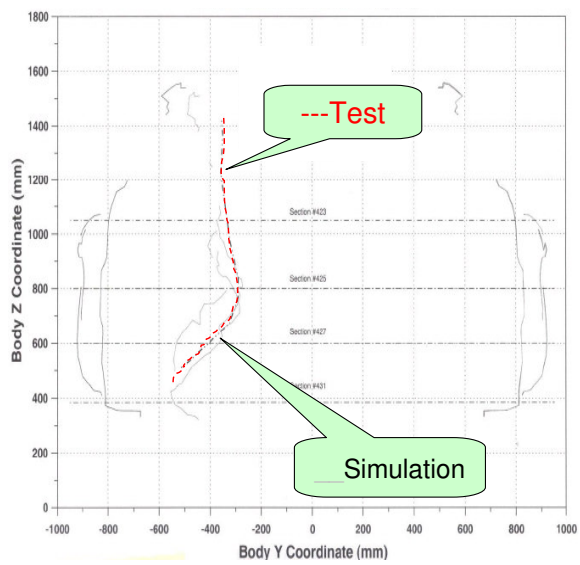

Figure 3. Intrusion comparison of struck vehicle in SUV-to-Car side impact.

3. DESIGN VARIABLE SELECTION

The appropriate selection of the striking vehicle design variables and the pertinent system responses are basic requirements. It is generally accepted that the determining factors of vehicle compatibility in frontal or side vehicle-to-vehicle impacts are relative geometry, relative stiffness, and relative mass. In this study, factors affecting the size and stiffness of the interaction zone were also considered. The following factors were considered as design variables for the striking vehicle (average SUV): front rail height, front rail thickness, vehicle mass, and bumper beam geometry (width and thickness).

Geometric difference between the SUV and the passenger vehicle was defined as the relative vertical alignment between the fore-most structural members (rails) and the struck vehicle's rocker. The SUV front-end stiffness was characterized through the front rail thickness. The bumper beam size and stiffness were also varied in front-to-side impacts. For each design variable, only the SUV portions of the FE models were allowed to vary within their respective ranges. A brief description of how the variables were introduced into the FE models and the levels selected for the design variables follows.

3.1 Geometry

In the baseline simulation both the SUV and the passenger car have the same ground reference plane The vertical alignment of energy-absorbing structures (rail) relative to the side of the passenger car was varied to four different levels by changing the ground reference plane of the SUV, as shown in Figure 4.

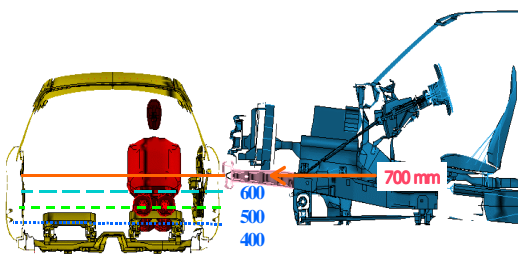

Figure 4. Levels of geometrical alignments of the SUV relative to the passenger car.

3.2 Stiffness

In general, thicknesses, cross section, and material strength, among other design parameters, determine the stiffness and the load carrying capacity of the front rail/frame of a vehicle. In this particular study, the cross section and material strength were kept as those of the baseline and thickness of the SUV rail was selected to be the stiffness-related deign variable. The thickness was studied at four distinct levels as indicated in Figure 5.

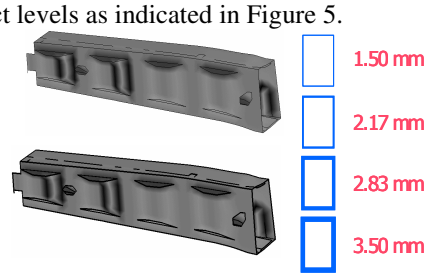

Figure 5. SUV rail and section thickness levels.

3.3 Mass Ratio

In order to vary the mass ratio of the impacted vehicles, the mass of the SUV was varied between baseline value less 13.5% to baseline value plus 24% in 227 kg increments. The SUV mass was adjusted by distributing small masses throughout the model such that the center of gravity location remained equivalent to that of the baseline model. This range approximately spans vehicle segments from small-size SUV to Mid-size SUV. Thus, the effect of the mass ratios was evaluated at four discrete levels (see Table 1).

Table 1. Passenger Vehicle and SUV Mass Levels

Struck Vehicle Mass (Kg)	Striking Vehicle Mass (Kg)	Striking/Struck Mass Ratio
1724	1680	0.97
1724	1906	1.11
1724	2133	1.24
1724	2360	1.37

3.4 Bumper Thickness and Width

Bumper size (expressed by its width in the vertical direction) and bumper metal thickness were considered as design parameters in this study. Three bumper width levels and four bumper metal thickness levels were selected to be evaluated for their effect on the struck vehicle occupant's TTI and Pelvis responses, as shown in Figure 6.

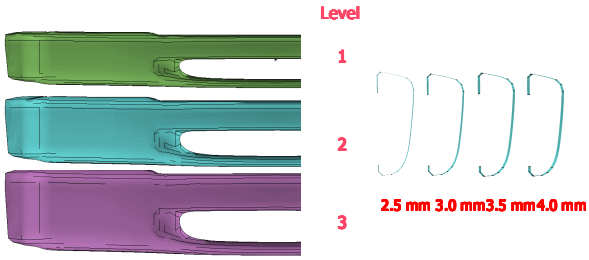

Figure 6. Bumper width and thickness levels.

Table 2 contains a summary of the design variables and their corresponding levels used in this study. The levels have been associated with an integer representation (coded) for simplicity.

Table 2: Coded Design Variables/Levels Summary

Rail Height
1=Ground to Rail Height 400 mm 2=Ground to Rail Height 500 mm 3=Ground to Rail Height 600 mm 4=Ground to Rail Height 700 mm
Mass
1=1680 kg 2=1906 Kg 3=2133 Kg 4=2360 Kg
Rail Thickness
1=1.5 mm 2=2.17 mm 3=2.83 mm 4=3.5 mm
Bumper Thickness
1=2.5 mm 2=3.0 mm 3=3.5 mm 4=4.0 mm
Bumper Height
1=1 2=2 3=3

4. SYSTEM RESPONSES

The struck passenger vehicle was stationary and contained the US side impact dummy (SID) in the driver seat, seated according to FMVSS 214. The striking SUV was given an initial velocity of 48 kph in the perpendicular direction to that of the side of the passenger vehicle. The SID dummy responses that were monitored in this study as system reponses were the Thoracic Trauma Index (TTI) and Pelvis acceleration.

5. EXPERIMENTAL DESIGN

The number of factors and levels included in this study describe a sizable design space. Numerous techniques exist for constructing experimental designs that specify a minimal number of samples throughout the design space required to characterize the responses [8, 9]. Latin Hypercube Sampling was utilized to select the levels for the design variable in the FE analyses. Since no noise factors were introduced into this study, total of 21 simulations were used to construct reasonably accurate response surfaces. The outcome of the sampling process is shown in Table 3. One additional run was included in the matrix to represent the baseline simulation that was correlated to a physical test for model validation. The corresponding matrix plot for all the five design variables used is shown in Figure 7.

Table 3. Design of Experiment Matrix

	Rail Height (mm)	Mass (kg)	Rail Thickness (mm)	Bumper Thickness (mm)	Bumper Width (Level)
Baseline	560	1906	3	3	2
1	400	1680	2.17	3	1
2	500	1680	1.5	3	3
3	600	1680	3.5	3	3
4	700	1680	2.17	3	1
5	400	1680	2.83	4	2
6	500	1906	3.5	4	1
7	600	1906	2.17	4	3
8	700	1906	1.5	2.5	2
9	400	1906	2.83	3.5	1
10	500	1906	3.5	2.5	3
11	600	2133	2.17	3.5	1
12	700	2133	1.5	3.5	2
13	400	2133	2.83	3	2
14	500	2133	3.5	4	2
15	600	2133	2.17	2.5	1
16	700	2360	1.5	2.5	3
17	400	2360	2.83	3.5	3
18	500	2360	3.5	2.5	1
19	600	2360	2.17	4	2
20	700	2360	1.5	3.5	2

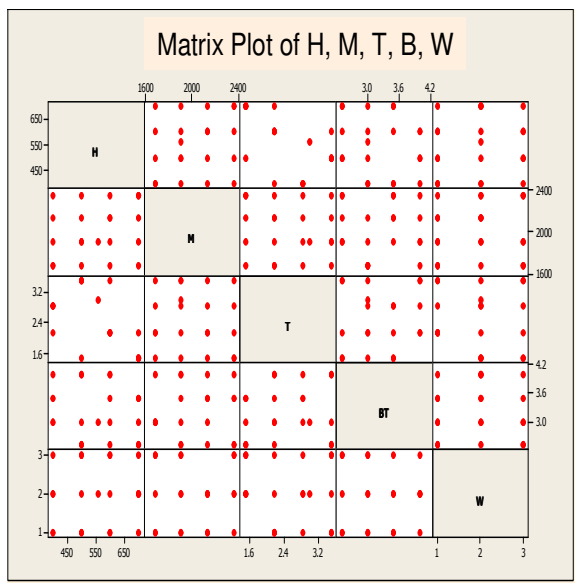

Figure 7. The DOE matrix plot.

6. FINITE ELEMENT SIMULATION RESULTS

Table 4 contains the dummy responses from all the 21 FE simulations. All dummy responses such as ribs and pelvis accelerations were normalized by their corresponding values obtained from the side impact baseline simulation. Values exceeding those obtained from baseline simulation are highlighted in yellow in Table 4. The TTI "Thoracic Trauma Index (TTI)" was calculated as the average of T12 and the maximum of the upper (U) or lower (L) rib accelerations.

7. RESPONSE SURFACE GENERATION AND PREDICTION EQUATIONS

The sample SID dummy responses of the TTI and pelvis acceleration obtained from the FE simulations (Table 4) were fitted with quadratic polynomials using a regression based upon subset selection by sequential replacement. These data were used to generate the response surfaces. The polynomial basis of the equations allows the response surface dependency on the design variables to be interpreted by observation. The response surfaces and R^2 values for the fitted polynomials are listed below. In the response surface expressions, H is the SUV rail height, T is the SUV rail thickness, M is the mass ratio, B is the bumper metal thickness, W is the bumper width in the vertical direction and a_1-a_6 and b_1.b_6 are the best fit coefficients

Table 4. Normalized Simulated Responses

	T12	U Rib	L Rib	TTI	Pelvis
base	1.00	1.00	1.00	1.00	1.00
1	1.08	0.65	0.84	0.94	1.89
2	0.87	0.86	0.79	0.82	1.01
3	1.12	1.38	1.06	1.11	1.04
4	0.99	1.25	1.15	1.08	0.63
5	0.88	0.73	0.70	0.78	1.67
6	1.05	1.01	0.95	0.99	1.23
7	1.11	1.25	0.98	1.05	1.05
8	0.95	1.23	0.90	0.97	0.66
9	0.95	0.70	0.63	0.77	1.51
10	0.96	0.93	0.80	0.87	1.19
11	1.00	1.10	1.00	1.00	0.88
12	0.96	1.58	1.06	1.13	0.58
13	0.89	0.73	0.69	0.78	1.70
14	0.88	0.80	0.75	0.81	1.05
15	1.03	1.11	1.00	1.01	0.71
16	0.95	1.49	1.10	1.09	0.59
17	0.88	0.79	0.78	0.82	1.66
18	0.95	0.83	0.97	0.96	1.16
19	0.97	1.10	1.31	1.17	1.01
20	1.00	1.30	0.97	1.02	0.51

$$TTI = a_1 - a_2.T^2 + a_3.M - a_4.M.T + a_5 H.T - a_6 H \quad \text{Eq.1}$$

$$(R^2 = 0.83)$$

$$Pelvis_Accel. = b_1 + b_2.H.T + b_3.B - b_4.T + b_5 H^2 + b_6 H \quad \text{Eq.2}$$

$$(R^2 = 0.93)$$

The coefficient of determination, referred to symbolically as R^2, is a measure of the model's ability to fit the specified regression curve and was used to quantify the quality of fit of the polynomial regression equation in a least squares sense. These coefficient of determination values (0.83 and 0.94) for the TTI and pelvis acceleration respectively indicate that the response surfaces are capable of representing the sampled FE results.

8. DISCUSSION OF RESULTS

Figures 8 and 9 show comparisons between FE simulation and predicted responses for normalized TTI and pelvis acceleration respectively. The comparison shows a good correlation between the simulated and predicted responses. Therefore, the response surfaces can be used with some confidence to predict occupant responses for other designs contained within the original design space of the design variables.

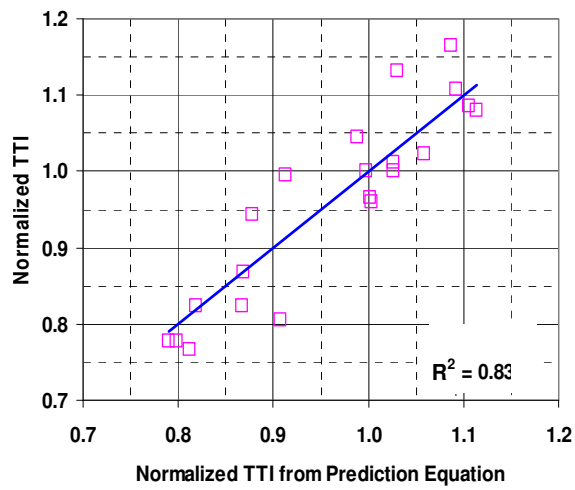

Figure 8. Normalized TTI from FE simulation versus that of prediction equation.

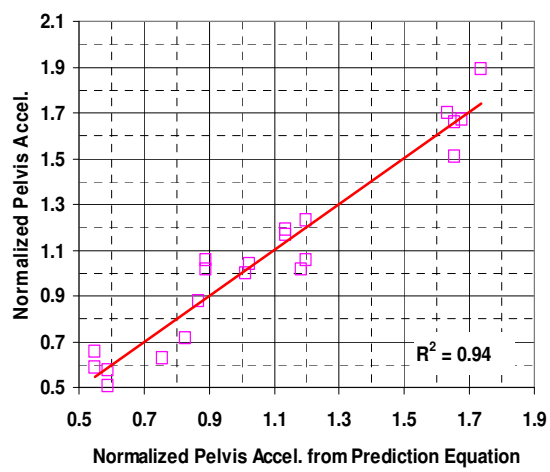

Figure 9. Normalized pelvis acceleration from FE simulation versus that of prediction equation.

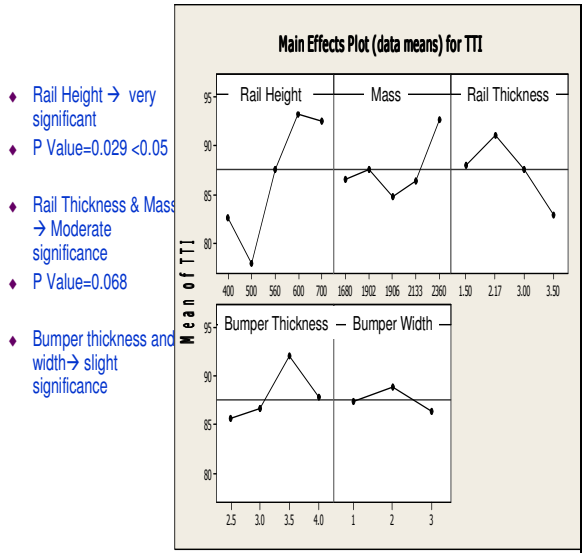

Figure 10. Main effect plot of design variables on TTI.

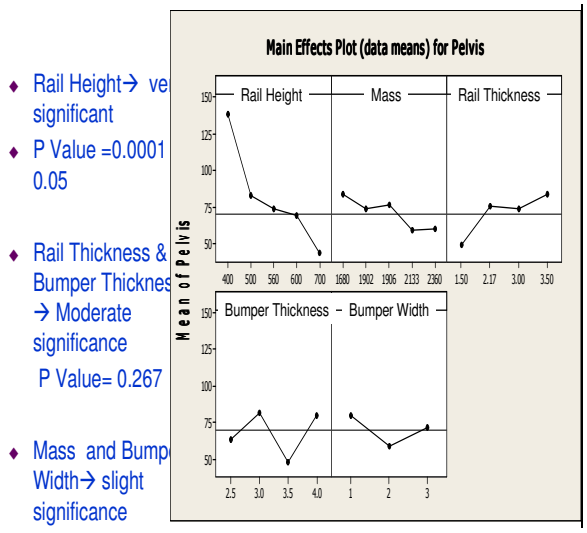

Figure 11. Main effect plot of design variables on pelvis acceleration.

Figures 10 and 11 show the main effects of the five design variables on dummy responses expressed by TTI and pelvis acceleration. The main effect plots indicate that both bumper width and bumper metal thickness have no significant effect on TTI and pelvis acceleration. This is also observed in the prediction equations (1) and (2) for TTI and pelvis acceleration respectively. The Plots also indicate that the rail/frame height from the ground reference has the most significant effect on the occupant's TTI and pelvis acceleration responses. The mass and stiffness have moderate significance.

9. PAIR-WISE COMPARISON OF DESIGN VARIABLE EFFECTS ON DUMMY RESPONSES

Pair-wise comparisons of the predicted effects of the design variables show the relative importance of each factor. For all comparisons described, the omitted variables were set to their baseline levels. Figure 12 shows the normalized TTI's response surface variation with rail height and rail thickness while the other design variables such as the mass, bumper width and bumper metal thickness were set to their baseline values. Similarly, Figure 13 shows the Normalized TTI's response surface variation with the rail thickness and striking vehicle mass while setting other design variable such as rail height, bumper width and bumper metal thickness to their baseline values. These figures show the dominant effect of the rail height on normalized TTI.

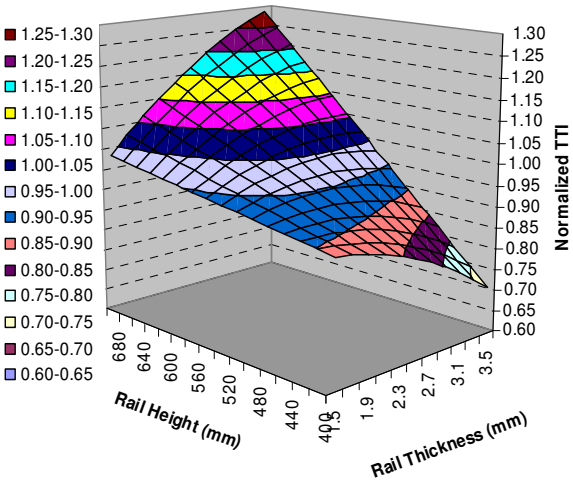

Figure 12. Normalized TTI response surface variation with rail height and rail thickness.

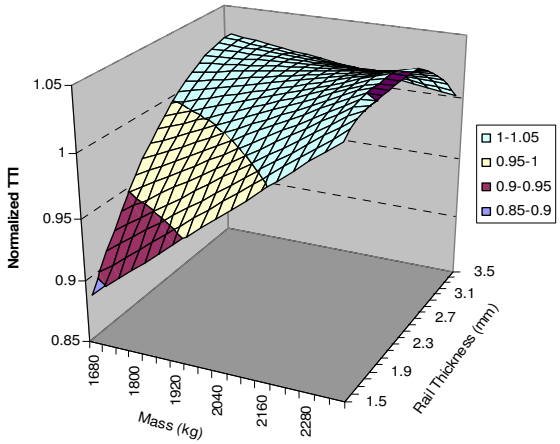

Figure 13. Normalized TTI response surface variation with mass and rail thickness.

In Figure 13 each color in the contours indicates a 5% change in effect. The normalized TTI can be reduced by 20% - 25% if rail height is reduced to the lowest level of 400 mm while keeping all the other four design variables the same as their baseline values. The response surface also shows an optimal design where the TTI can be reduced by 30% can be achieved by setting the rail height to the lowest of 400mm while increasing the rail thickness from the baseline by approximately 16% (baseline thickness of 3mm increase to 3.5 mm). This makes sense because slightly stiffer rail contacting the struck passenger car's area near stiff rocker dissipates more of the impact energy of the striking SUV through near rocker and rocker deformation.

The result achieved in this CAE based study appears to be very consistent with field data and real world performance as indicated in recent IIHS study on crash compatibility between cars and light trucks, Baker et. al. [10]. Their study focused on real world benefit achieved by lowering front-end energy-absorbing structure (rails) in SUV's and pickups. In their study only recent SUVs and pickup trucks of model years 2000 through 2003 were included for both front-to-front and front-to-side collisions (where the front end of a light truck strikes the driver side of a passenger car). In front-to-side impacts, a 30% risk reduction for SUVs and a 10% risk reduction for pickups are observed with SUVs complying vehicles with the Phase I Front-to-Front Compatibility Alliance Voluntary Standard [11].

Figure 13 shows that the optimum design can only lead to approximately 11% reduction in TTI even the striking SUV mass and rail thickness are set to their minimum values of 1680 Kg and 1.5 mm respectively. This also emphasize the fact that the most significant design variable effect on the TTI is the rail height.

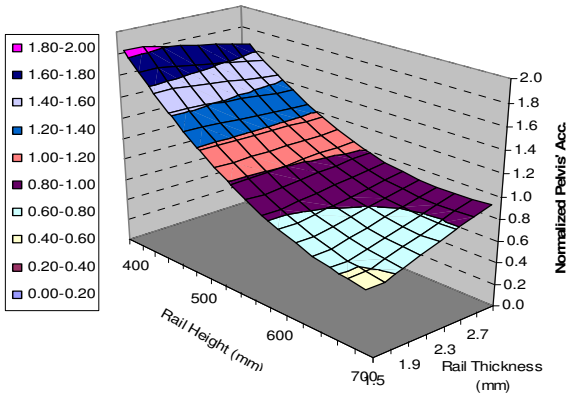

Figure 14. Normalized pelvis response surface variation with rail height and rail thickness.

Figure 14 shows the normalized pelvis acceleration's response surface variation with the rail height and rail thickness. Other design variables such as the mass, bumper width and bumper metal thickness were set to their baseline values. Each color in the contours indicates a 20% change in effect. The rail height shows its dominant effect on reducing pelvis acceleration when it is set to its highest level but it has an adverse effect on increasing the TTI. In other words, reducing the rail height to 400mm to achieve approximately 30% reduction in TTI will increase pelvis acceleration by approximately 60% (see color contours in Figure 14). However, the baseline run resulted in a very low pelvis acceleration value of approximately 44% below the IARV (Injury Assessment Reference Value). This points to a tradeoff between the TTI and pelvis acceleration when considering rail height changes.

As it is shown in Eq. (2), the mass effect did not appear in the prediction equation for pelvis acceleration, which means it has no significant effect on pelvis acceleration. These results are also consistent with conclusions found in other studies by Nolan et. al. [3] in laboratory testing. In their test series, it was shown that a 15% increase in the mass of the striking SUV has no significant effect on pelvis acceleration of the driver occupant of the struck passenger car.

10. SUMMARY

- Validated finite element models of an "average" SUV and an "average" passenger vehicle were used to explore the effects of geometry, stiffness and mass in front-to-side impact simulations.
- A design of experiments methodology involving Latin Hypercube sampling was employed to select the appropriate number of simulations and the design levels of each of the design variables that should be incorporated in each simulation.
- Five design variables, the SUV rail height, rail thickness, mass, bumper width and bumper metal thickness were chosen.
- Thoracic Trauma Index (TTI) and pelvis acceleration of the SID dummy responses were selected for the system responses. These responses were normalized by their baseline corresponding values.
- The main effect plots were generated to identify the significance of individual design variable. The responses were characterized by quadratic polynomial surfaces.
- Pair-wise comparisons of the effects of the design variables were used to assess their

individual influence on TTI and pelvis acceleration. The pair-wise comparisons were based on the response surfaces generated from the 21 FE simulations. When a pair of design variables was compared, the remaining design variables were set to their BASELINE levels.

11. CONCLUSIONS

- A good correlation of the normalized dummy responses, TTI and Pelvis acceleration, between the values obtained from the FE simulations and those obtained from the prediction equations were achieved.
- The Main Effect Plots indicated that in front-to-side impacts of an SUV to a passenger car the geometrical effect, characterized by rail/frame height from the ground reference, on the normalized TTI and pelvis acceleration is most significant.
- The stiffness and mass effects on the normalized TTI response were identified to be of some significance, however, the geometry or the rail/frame height effect dominated the outcome. It should be emphasized that changing the rail thickness of the striking vehicle will affect its frontal crashworthiness. This effect has not been investigated in this study.
- The significant effect of geometry obtained through this CAE based study is consistent with field data and real world performance as indicated in recent IIHS study on crash compatibility between cars and light trucks [10]
- The main effect plots indicated that bumper width and bumper metal thickness have no significant effect on neither the normalized TTI nor the normalized pelvis acceleration.
- The normalized TTI response was seen to increase with striking vehicle rail height, mass and stiffness, but the response of normalized dummy pelvis was seem to be only sensitive to the striking vehicle's rail height. The mass has no significant effect on the normalized pelvis acceleration. This finding is also consistent with laboratory findings from crash testing conducted by IIHS [3]

12. REFERENCES

[1] Hollowell, W.T. and Gabler, H.C. 1996. “NHTSA’s Vehicle Aggressivity and Compatibility Research Program.” 15th ESV, Paper No 96-S4-O-01, Melbourne, Australia.

[2] Lugt, D.V., Connoly, T., and Bhalsod, D. 1999. "Vehicle Compatibility – Analysis of the Factors Influencing Side Impact Occupant Injury" SAE 1999-01-0067.

[3] Nolan, J., Powell, M., Preuss, A., and Lund, A. 1999." Factors Contributing to Front-Side Compatibility: A Comparison of Crash Test Results." 1999, Stapp Conference, 99SC02.

[4] Barbat, S., Li, X., and Prasad, P. 2001. "A Comparative Analysis of Vehicle-to-Vehicle and Vehicle-to-Rigid Fixed Barrier Frontal Impact." 17th ESV, Paper No. 01-S7-O-01, Amsterdam, Netherlands.

[5] Barbat, S., Li, X., and Prasad, P. 2001. "Evaluation of Vehicle Compatibility in Various Frontal Impact Configurations ." 17th ESV, Paper No. 01-S7-O-09, Amsterdam, Netherlands.

[6] Barbat, S., Li, X., Przybylo, P., and Prasad, P. 2003. "Vehicle-to-Vehicle Full Frontal Crash Optimization Using a CAE-Based Methodology." 18th ESV, Paper No. 05-S7-O-145, Nagoya, Japan.

[7] RADIOSS Crash Guidelines, Mecalog SARL, 1997.

[8] Yang, R.J., Akkerman, A., Anderson, D., Faruque, O., and Gu, L. 2000. "Robustness Optimization for Vehicular Crash Simulations." Computing in Science and Engineering.

[9] Gu, L. 2001. "A Comparison of Polynomial-based Regression Models in Vehicle Safety Analysis." ASME 2001 DETC, Paper No. DAC-21063, Pittsburgh.

[10] Baker, B,. Nolan, J., O’Neill, B., Genetos, A. 2007. “Crash Compatibility between Cars and Light Trucks: Benefits of Lowering Front-End Energy-Absorbing Structure in SUV’s and Pickups.” Insurance Institute for Highway Safety, Arlington, VA.

[11] Auto Alliance, December, 2003. “Enhanced Vehicle-to-Vehicle Crash Compatibility: Commitment for Continued Progress by Leading Automakers".

A STUDY ON AHOF400 WHICH IS POSSIBLE CAR TO SUV COMPATIBILITY EVALUATION METHOD

Hayata Uwai
Shinkichi Toyosaki
Koichi Sagawa
Nobuhiko Takahashi
Nissan Motor Co., Ltd.
Japan
Paper Number 07-0391

ABSTRACT

Research on the evaluation method for vehicle compatibility has continued among passive safety industries in recent years. NHTSA, which has jurisdiction over automobile safety in the U.S., is studying AHOF400 as a new criteria to evaluate interaction between vehicles to improve compatibility performance. In this paper, the target value of AHOF400 was assumed to be Part581 zone, which is the front bumper height of a passenger car. A basic study was carried out using finite element modeling of an existing vehicle model and a real vehicle crash test in order to determine how to practically modify the vehicle structure of an SUV. As a result, it was determined that the height of the Front Side Member of an SUV should be lower than that of a passenger car in some cases. This is different from the original aiming point that car-to-car interaction would be improved by restriction of AHOF400, which makes the height of front end structures the same level. As a way to solve the concern, an evaluation area of barrier load cells height which is appropriate to calculate AHOF400 was studied

INTRODUCTION

Vehicle safety performance was enhanced by regulations and crash test publication, in addition to continuous effort by car manufactures for many years. Especially Self Protection performance during a crash has been improved very well. In addition, safety concept to reduce the aggressiveness to vehicles and passengers during car-to-car accident is being expanded. And optimization of self protection and partner protection is known as an approach to enhance passive safety performance. This kind of approach is called compatibility generally.
Recently the selling volume of sport utility vehicles (SUV) and light track vehicles (LTV) is being increased, therefore aggressiveness of SUV and LTV against passenger vehicle is pointed out. For example, Mr Kahene reported that LTV is more aggressive than passenger vehicle in case of full lap and offset crash in car-to-car crash, in the report by The National Highway Traffic Safety Administration (NHTSA) in 2003 **[1]**. And compatibility of Car to SUV or LTV is under research by NHTSA **[2, 3 and 4]** and The Insurance Institute of Highway Safety (IIHS).
Generally, basic idea to improve compatibility performance is considered to be followings **[5]**.
1)Increasing interaction of front end structure between vehicles
2)Matching the load between vehicles
Based on this idea, NHTSA is studying 1) Regulation regarding Average Height of Force of front end structure (AHOF400) to increase interaction between vehicles, 2) Front end load (KW400) to match the balance between vehicles as an regulation **[6]**. According to basic research by NHTSA, AHOF400 and KW400 of SUV and LTV are more than the upper limit of criteria which was recommended by NHTSA **[7]**, therefore it is presumed that the additional modification of front end structure of SUV and LTV is needed from now.
From such a background, basic research about AHOF400 was carried out in this paper. Basic study by the FEM simulation using existing car and a vehicle test were carried out to understand how body structure should be modified practically to achieve NHTSA concept, in case of SUV which the aggressiveness against a passenger car is concern especially.

CALCULATION METHOD OF AHOF400 (AVERAGE HEIGHT OF FORCE)[6]

The followings is a summary of the calculation method of AHOF400. AHOF400 is an index which shows the Average Height of Force of the front part of a vehicle when vehicle deformation is 400mm, and it is calculated by using the output value from the barrier load cell on a rigid barrier in 35MPH full overlap crash test. Load cells are set on the rigid barrier in 10 lines and 16 rows, the size of each load

cell width is 125mm by 125mm, the height of lower edge is 80mm and upper edge of load cell is 1330mm from the ground. AHOF400 is computed by using Equitation (1) and (2).

The aiming point is that front structure (i.e. Front Side Member) of various type of vehicle should be in same level of ground height and vehicle interaction can be improved, by limiting upper and lower value of AHOF400. Recently, making the main front end structure distributed around the height of the bumper on passenger vehicles (Part581 zone; 406 to 508mm) is under study. Therefore, target of AHOF400 criteria was assumed to be within Part581 zone, in this paper.

$$AHOF400 = \frac{\int_0^{400} F(s)COF(s)ds}{\int_0^{400} F(s)ds} \quad (1).$$

$$COF(s) = \frac{\sum H_i f_i(s)}{\sum f_i(s)} \quad (2).$$

COF(s) : Center of Force

F(s) : =Σfi(s)

fi(s) : Force on each load cell

Hi : Height of each load cell

BASIC STUDY OF AHOF400 BY FRONTAL CRASH SIMULATION USING FINITE ELEMENT METHOD

The crash simulation was carried out by using FEM model of an existing car to understand how the structure should be modified practically to achieve the assumed criteria of AHOF400, especially in the case of a collision with an SUV. Because the Front Side Member most greatly influences the results, its height was the focus of the study.

PAM-CRASH was used as the solver of the simulation. The model showed in Figure 1. Moreover AHOF400 from physical vehicle test and the above-mentioned crash simulation results were compared to confirm analytical accuracy (Table 1). Because AHOF400 calculated from the FEM simulation are lower than result of vehicle tests as a trend, the numerical value of AHOF was corrected in the ratio of the physical vehicle test results and simulation results, was used in this paper. (Table 1)

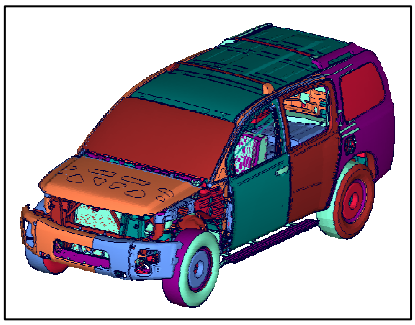

Figure 1. Simulation model.

Table 1.
Difference between AHOF400 calculated from crash test and simulation results

	Experiment	Analysis
AHOF400[mm]	592	578

The relationship between AHOF400 and the height of the Front Side Member by simulation is shown in Figure 2. In the case of the model, where the height of the Front Side Member is higher than Part581 zone in a simulation; the AHOF400 value is much higher than the assumed upper limit (Figure 2-(a)). If the height of Front Side Member is in the middle area of Part581 zone, AHOF400 is still higher than the assumed upper limit (Figure 2-(b)). As a result, height of Front Side MBR has to be lower than Part581 zone to use current AHOF as a recommendation. Figure 3 shows the barrier load distribution when the amount of the body deformation is 400mm. It is understood the main load that influences AHOF400 by the time body deformation is 400mm is generated at the following position; bonnet hood (Figure 3-(a)), front end composition parts in front of the engine (Figure 3-(b)) and Front Side Member (Figure 3-(c)).

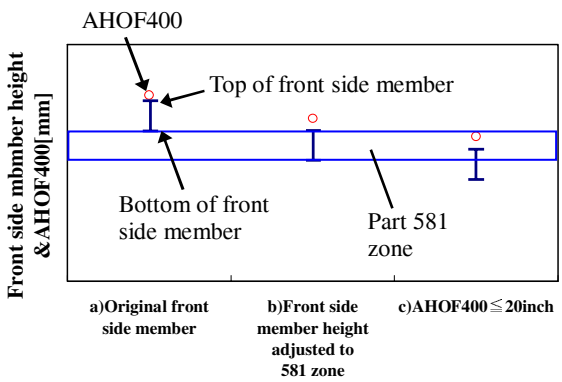

Figure 2. Relationship between front side member height and AHOF400.

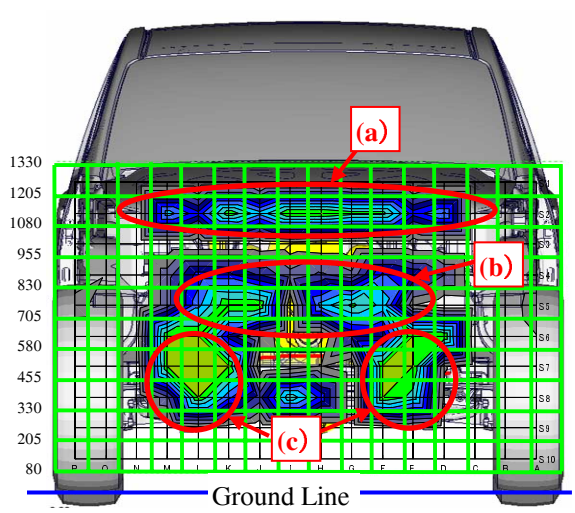

Figure 3. Relationship between barrier load and structure layout

The aim of the AHOF400 restriction is distributing Front Side Member of various types of cars around the Part581 zone to improve the interaction of front end structure between vehicles. This analysis result shows that the Front Side Member becomes lower than Part581 zone in this case, even if it suits the AHOF400 to Part581 zone, unlike the above-mentioned aim (Figure 4). The main cause is considered to be load by the structural element around bonnet hood. Although the load around the hood is low as compared to the Front Side Member load, since road clearance is high, it is presumed as a factor which makes AHOF400 increase (Fig. 3- (a), (c)). Then, in order to check the influence on AHOF400 by the load around the hood, a crash simulation was carried out without a hood, as shown in Fig. 5. As a result, AHOF400 increased 40mm with a hood, and the influence of the hood on AHOF was understood (Table 2).

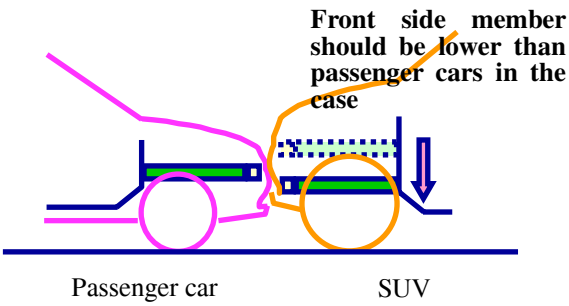

Figure 4. Front Side Member relation between SUV and passenger car to meet AHOF400

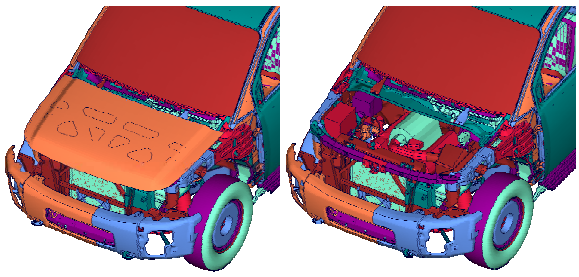

a)With hood b)Without hood

Figure 5. Simulation model with/without hood

Table 2.
Difference AHOF400 with and without hood (simulation results)

	With hood	Without hood	Difference
AHOF400 [mm]	489	449	-40

STUDY OF AHOF400 IN CASE OF RESTRICTED BARRIER LOAD CELL EVALUATION AREA

From the basic study about AHOF400 in the preceding chapter, AHOF400 is increased from the influence of structure like as a bonnet hood which position is higher than Front Side Member height. It has been found out that the AHOF400 cannot achieve Part581 zone, if the Front Side Member is not lower than the lower limit of the Part581 zone.
Generally, in a Car to SUV/LTV head-on collision by which the aggressiveness of SUV and LTV is regarded as a concern, the structure around the bonnet hood of SUV/LTV does not overlap the front part of a passenger car in the height direction (Fig. 6), therefore it is hard to think that it has a big influence on the interaction between passenger vehicles and SUV/LTV. It is considered as one of the subjects of AHOF400 that AHOF400 of SUV and LTV increases with such a structural element considered that the influence of the interaction between vehicles is small.

Figure 6. Relation of the front structural element and passenger car and SUV.

In this paper, how to eliminate the load of the structure of an SUV/LTV which is not overlapped with the front end of a passenger car in AHOF400 calculation was studied as a proposal. As a concrete method, the influence of the structure which is not overlapped with the front of a passenger car in vertical direction can be eliminated by making the barrier load cell height lower than 1330mm in AHOF400 calculation. In this paper, new barrier load cell evaluation range is defined from the two following viewpoints.

Height of front part of passenger car

Here, because AHOF400 is calculated at the time of 400mm of body deformation, the front part height of the passenger car was defined as the height of the hood, which is 400mm rearward from the front end of a passenger car (Fig. 7). The distribution of height of the front part of passenger car is shown in Fig. 8. Fig. 8 shows that the height of the front part of passenger car is on 850mm or less.

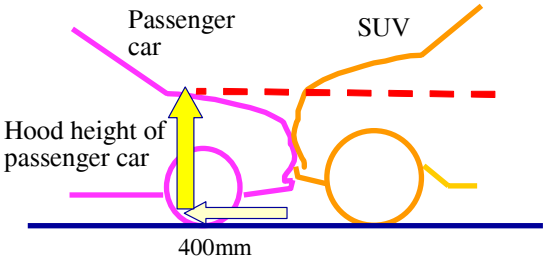

Figure 7. Height of front part of passenger car.

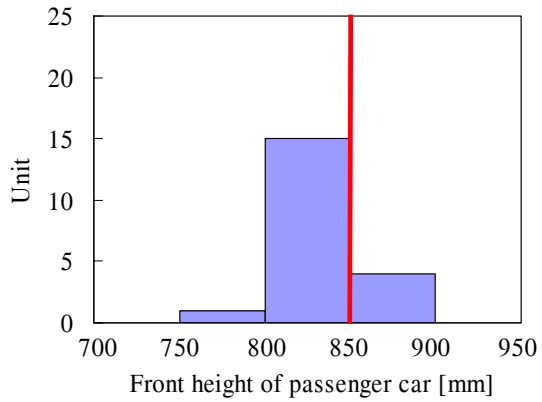

Figure 8. Hood height of passenger vehicles.

Barrier height which imitated the passenger car used in crash tests

Table 3 shows the height of the barrier that imitates passenger cars which are used in the front crash test of North America, the side impact regulation, and the assessment test of each country. It shows that each barrier height is distributed within 800-850mm.

Table 3.

Barrier height used in crash tests in each country

UNIT[mm]	Frontal Impact		Side Impact	
REGION	Regulation	Information Disclosure	Regulation	Information Disclosure
US	850	850	839	839
JPN	-	850	800	800
EUR	850	850	800	800

From the two above-mentioned viewpoints, 830mm (Fig. 4), which is a barrier load cell boundary position between the road clearances of 800-850mm, was made the upper limit of the evaluation area.
AHOF400 calculated by the above-mentioned method is shown in figure 9-(d). In this case, the Front Side Member height that meets Part581 zone, which is the assumed target of AHOF400, was distributed over Part581 zone. This result approached the aim of distributing the frontside member of an SUV over Part581 zone, which is the bumper height of a passenger car. Moreover, the same tendency was seen also in the physical vehicle test result (Fig. 10).

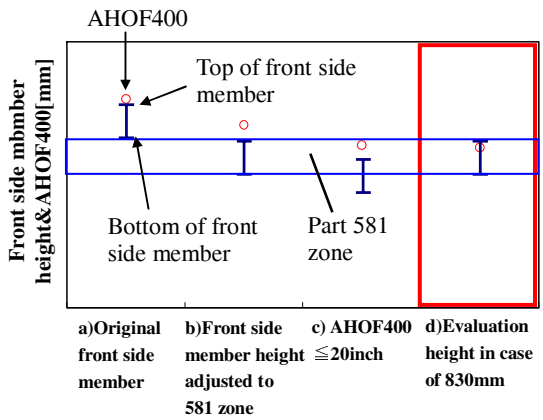

Figure 9. Relationship between AHOF400 and new evaluation method.

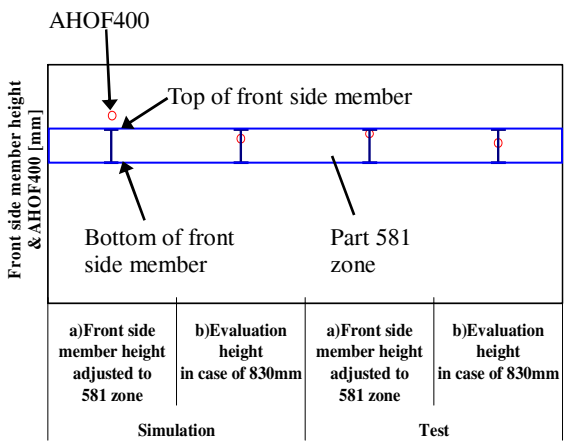

Figure 10. Relationship between AHOF400 and new evaluation method in vehicle crash tests.

CONCLUSIONS

In attempting to achieve the assumed target of AHOF400, which is part581 zone, there are cases where it cannot be achieved if the Front Side Member of an SUV/LTV is not made lower than a passenger car's. This view is different from the original aim, which was to improve the interaction between vehicles by making the height of various types of front structures a fixed height by regulating AHOF400. As a possible cause, the influence of a structure such as the hood, which is not overlapped with the front of a passenger car in the vertical direction, was considered. The upper limit of the AHOF400 evaluation area was restricted to the same height as passenger cars in this study. As a result, it was found out that the original aim can be achieved.

REFERENCES

[1] Kahane, C., "Vehicle Weight, Fatality Risk and Crash Compatibility of Model Year 1991-99 Passenger Cars and Light Trucks", October 2003, DOT HS 809 662.

[2] Hollowell, W.T. and Gabler, H.C. "NHTSA's Vehicle Aggressivity and Compatibility Research Program", 15th International Conference on the Enhanced Safety of Vehicles, Paper No. 96-S4-O-01, Melbourne, Australia, 1990.

[3] Gabler, H.C. and Hollowell, W.T., " The Aggressivity of Light Trucks and Vans in Traffic Crashes", SAE Paper No. 980908, Detroit, 1998.

[4] Summers, S., Prasad, A. and Hollowell, W.T., "NHTSA's Vehicle Compatibility Research Program", SAE Paper No. 1999-01-0071, Detroit, 1999.

[5] Edwards, M., et al., "Development of Test Procedures and Performance Criteria to Improve Compatibility in Car Frontal Collisions.", Vehicle Safety 2002.

[6] David L. Smith, "NHTSA Compatibility Research Update", SAE Government/Industry Meeting, 2006